

See discussions, stats, and author profiles for this publication at: <https://www.researchgate.net/publication/270513987>

# SMAD4 exerts a tumor-promoting role in hepatocellular carcinoma

Article in *Oncogene* · December 2014

DOI: 10.1038/onc.2014.425 · Source: PubMed

CITATIONS

34

READS

342

20 authors, including:



**Pratika yuhyi Hernanda**

Universitas Wijaya Kusuma Surabaya

12 PUBLICATIONS 105 CITATIONS

[SEE PROFILE](#)



**Kan Chen**

Erasmus MC

25 PUBLICATIONS 268 CITATIONS

[SEE PROFILE](#)



**Asha Das**

National Center for Tumor Diseases (NCT) Heidelberg

17 PUBLICATIONS 190 CITATIONS

[SEE PROFILE](#)



**Kostandinos Sideras**

Erasmus MC

56 PUBLICATIONS 1,718 CITATIONS

[SEE PROFILE](#)

Some of the authors of this publication are also working on these related projects:



mesenchymal stem cell [View project](#)



Barrett's Esophagus [View project](#)

## ORIGINAL ARTICLE

## SMAD4 exerts a tumor-promoting role in hepatocellular carcinoma

PY Hernanda<sup>1,2,8</sup>, K Chen<sup>1,3,8</sup>, AM Das<sup>4,8</sup>, K Sideras<sup>1,8</sup>, W Wang<sup>1</sup>, J Li<sup>1</sup>, W Cao<sup>1</sup>, SJA Bots<sup>1</sup>, LL Kodach<sup>1</sup>, RA de Man<sup>1</sup>, JNM Ijzermans<sup>5</sup>, HLA Janssen<sup>1,6</sup>, AP Stubbs<sup>7</sup>, D Sprengers<sup>1</sup>, MJ Bruno<sup>1</sup>, HJ Metselaar<sup>1</sup>, TLM ten Hagen<sup>4</sup>, J Kwekkeboom<sup>1</sup>, MP Peppelenbosch<sup>1</sup> and Q Pan<sup>1</sup>

Further understanding of the molecular biology and pathogenesis of hepatocellular carcinoma (HCC) is crucial for future therapeutic development. SMAD4, recognized as an important tumor suppressor, is a central mediator of transforming growth factor beta (TGFB) and bone morphogenetic protein (BMP) signaling. This study investigated the role of SMAD4 in HCC. Nuclear localization of SMAD4 was observed in a cohort of 140 HCC patients using tissue microarray. HCC cell lines were used for functional assay *in vitro* and in immune-deficient mice. Nuclear SMAD4 levels were significantly increased in patient HCC tumors as compared with adjacent tissues. Knockdown of SMAD4 significantly reduced the efficiency of colony formation and migratory capacity of HCC cells *in vitro* and was incompatible with HCC tumor initiation and growth in mice. Knockdown of SMAD4 partially conferred resistance to the anti-growth effects of BMP ligand in HCC cells. Importantly, simultaneous elevation of SMAD4 and phosphorylated SMAD2/3 is significantly associated with poor patient outcome after surgery. Although high levels of SMAD4 can also mediate an antitumor function by coupling with phosphorylated SMAD1/5/8, this signaling, however, is absent in majority of our HCC patients. In conclusion, this study revealed a highly non-canonical tumor-promoting function of SMAD4 in HCC. The drastic elevation of nuclear SMAD4 in sub-population of HCC tumors highlights its potential as an outcome predictor for patient stratification and a target for personalized therapeutic development.

*Oncogene* advance online publication, 22 December 2014; doi:10.1038/onc.2014.425

## INTRODUCTION

SMAD proteins are recognized as central mediators of transforming growth factor beta (TGFB) and/or bone morphogenetic protein (BMP) signaling pathways, which regulate a plethora of physiological processes including cell growth and differentiation.<sup>1</sup> Accordingly, deregulation of TGFB/BMP pathways almost invariably leads to developmental defects and/or diseases, in particular cancer.<sup>2</sup> These two pathways signal through the family of SMAD proteins to exert their effects. In mammals, there are eight SMADs that are subdivided into three distinct classes: receptor-regulated SMADs (R-SMADs) comprising SMAD2 and SMAD3 (transduce TGFB signaling) and SMAD1, SMAD5 and SMAD8 (transduce BMP signaling); a common SMAD called SMAD4; and two inhibitory SMADs, namely, SMAD6 and SMAD7.<sup>3</sup> SMAD proteins are highly conserved within their family and across species, with SMAD4 representing a somewhat divergent subtype, which still retains about 40% identity with other family members.<sup>4</sup> SMAD4 binds to R-SMADs and forms heteromeric complexes and facilitating the translocation of these heteromeric complexes into the nucleus. In the nucleus, the heteromeric complex binds to promoters and interacts with transcriptional activators<sup>2,5</sup> and the presence of nuclear SMAD4 protein has profound consequences for gene expression.

Originally identified as a candidate tumor-suppressor gene at 18q21.1 decades ago,<sup>6</sup> the tumor-suppressive function of SMAD4 has now almost achieved dogmatic status and loss of its activity has been implicated in the initiation and progression of a multitude of cancer types.<sup>2,7–10</sup> Loss or inactivation of both normal gene copies is associated with carcinoma in several organ systems, including approximately 55% of pancreatic adenocarcinomas,<sup>6</sup> 15–55% of extrahepatic cholangiocarcinomas<sup>11</sup> and a smaller percentage of gastrointestinal and other carcinomas.<sup>12,13</sup> Strikingly, loss of SMAD4 expression in hepatocellular carcinoma (HCC) has not been observed, prompting investigations into role and importance of this tumor suppressor in this disease. Hence, we endeavored to establish the role of SMAD4 in HCC, which we uncovered a non-conventional function of SMAD4 in HCC as a tumor promoter.

## RESULTS

SMAD4 gene mutation is rare in HCC patients but its mRNA expression is significantly upregulated in the tumor tissue. As SMAD4 genomic alterations have been reported for several cancers, we have attempted to analyze its genomic abnormalities

<sup>1</sup>Department of Gastroenterology and Hepatology, Erasmus MC Cancer Institute, Erasmus University Medical Center and Postgraduate School Molecular Medicine, Rotterdam, The Netherlands; <sup>2</sup>Laboratory of Medical Genetics, Biomolecular Research Centre, Wijaya Kusuma University, Surabaya, Indonesia; <sup>3</sup>Bio-X Center, College of Life Sciences, Zhejiang Sci-Tech University, Hangzhou, China; <sup>4</sup>Laboratory of Experimental Surgical Oncology Section Surgical Oncology, Department of Surgery, Erasmus University Medical Center, Rotterdam, The Netherlands; <sup>5</sup>Department of Surgery, Erasmus University Medical Center, Rotterdam, The Netherlands; <sup>6</sup>Division of Gastroenterology, University Health Network, Toronto, Ontario, Canada and <sup>7</sup>Department of Bioinformatics, Erasmus University Medical Center, Rotterdam, The Netherlands. Correspondence: Dr Q Pan, Department of Gastroenterology and Hepatology, Erasmus MC Cancer Institute, Erasmus University Medical Center and Postgraduate School Molecular Medicine, Room Na-617, 'sGravendijkwal 230, NL-3015 CE Rotterdam, The Netherlands.

E-mail: q.pan@erasmusmc.nl

<sup>8</sup>These authors contributed equally to this work.

Received 21 July 2014; revised 7 November 2014; accepted 18 November 2014

in patient HCC tissues. We have searched the database of the cBioPortal for Cancer Genomics. We identified three cohorts of total 457 HCC patients with genomics data of *SMAD4* gene (Figure 1a). There are only two patients identified to harbor mutations (R87W; A462T), suggesting that *SMAD4* gene mutation in HCC is rather rare, in contrast to pancreatic or colorectal cancers (up to 20–30%) (Figure 1a). In addition, one HCC patient was found to have *SMAD4* gene amplification and another one has *SMAD4* deletion (Figure 1a).

We further searched the Oncomine microarray database to analyze mRNA expression of *SMAD4* in patient HCC. In total, we have identified five cohorts of 424 HCC tissue samples compared with 344 liver tissues. *SMAD4* mRNA was upregulated in all the cohorts. By polling all the cohorts, there is a significant increase of *SMAD4* mRNA expression in the HCC tumor compared with liver tissue ( $P < 0.05$ ) (Figure 1b). These data indicate that genomic alteration is rare but elevation of mRNA expression is common in patient HCC tumor.

Drastic elevation of nuclear *SMAD4* expression in the tumors of sub-population of HCC patients

The paucity of data surrounding the functionality of *SMAD4* in HCC prompted us to analyze *SMAD4* expression and activation in a panel of resected HCC from 140 individual patients and compare the results with adjacent non-transformed tissue. In these patients, nuclear *SMAD4* protein (Figure 2a) was taken as measure of *SMAD4* signaling activity, as it is generally assumed that this fraction of the *SMAD4* pool represents the transcriptionally active form of the protein. The staining was scored by two independent investigators with a Kappa test of 0.773, suggesting that there was an excellent agreement in scoring between the two investigators. The levels of *SMAD4* protein positivity range from low (score: 0–<2), moderate (score: 2–<3) to high (score: 3–4) both in the HCC tumors and their adjacent sites (Figures 2a and b). Interestingly, nuclear *SMAD4* levels were considerably higher in human HCC tissue as compared with normal adjacent liver tissue ( $n = 140$ ,  $P < 0.01$ ) (Figures 2a and c), which is consistent with the upregulation of mRNA expression in HCC (Figure 1b). Subsequent subgroup analysis according to the nuclear *SMAD4* score in the tumor showed that there was no difference of *SMAD4* levels between tumor and adjacent tissue in patients displaying low-to-moderate nuclear *SMAD4* scores ( $n = 97$ , data not shown); whereas a drastic elevation was observed in tumor compared with adjacent tissue in the high *SMAD4* expression group, ( $3.47 \pm 0.45$  vs  $2.27 \pm 0.92$ , mean  $\pm$  s.e.m.,  $n = 43$ ,  $P < 0.001$ ) (Figure 2c).

Analysis focusing on clinical behavior of the cancer (Supplementary Table S1) revealed that high levels of nuclear *SMAD4* were not significantly associated with tumor size ( $n = 98$  analyzable patients), number of tumor lesions ( $n = 129$  analyzable patients) and vascular invasion ( $n = 78$  analyzable patients), but significantly associated with higher levels of alpha-fetoprotein pre-resection ( $n = 135$  analyzable patients,  $P < 0.01$ ). Serum alpha-fetoprotein has been suggested as an independent indicator for HCC prognosis and patients with high alpha-fetoprotein levels have been reported to have shorter survival.<sup>14</sup> In addition, *SMAD4* is significantly associated with fibrosis ( $P < 0.01$ ) (Supplementary Figure S1). Liver fibrosis is in turn strongly correlated with HCC development.<sup>15</sup> Furthermore, nuclear *SMAD4* level was significantly higher in undifferentiated tumor than in well-differentiated tumor of HCC ( $2.53 \pm 0.23$  vs  $1.94 \pm 0.11$ , mean  $\pm$  s.e.m.,  $n = 127$ ,  $P < 0.05$ ) (Figure 2d).

Importantly although, apparently high *SMAD4* positivity in surgically resected HCC ( $n = 130$  analyzable patients) tend to have higher risk of fast recurrence (hazard ratio (HR) = 1.420, 95% confidence interval (CI): 0.711–2.836 in the high-level group) and higher risk of poor survival (HR = 1.844, 95%CI: 0.894–3.803 in

the high-level group) (Figures 2e and f). Kaplan–Meier analysis ( $n = 130$  analyzable patients) also indicated a trend of shorter time to recurrence and lower cumulative survival in high *SMAD4* level patients, although not statistically significant (Figures 2e and f). We interpreted that higher nuclear *SMAD4* levels may be associated with more aggressive types of tumors in HCC patients.

Silencing of *SMAD4* expression reduced colony formation in human hepatoma cell lines

In order to obtain an insight into the mechanisms possibly mediating the negative relation between *SMAD4* signaling and HCC clinical behavior, we used lentiviral RNA interference vectors expressing short hairpin RNA (sh-*SMAD4*) to stably knockdown *SMAD4* expression in human HCC cell lines and subsequently characterized the cellular consequences thereof. Supplementary Figure S2 showed the efficacy of gene silencing using this strategy. A vector expressing short hairpin RNA targeting green fluorescent protein served as control (CTR). The success of this approach was confirmed by western blot and probing for *SMAD4* protein (Figure 3a), which showed almost absence of the protein in the knockdown cell lines, whereas the control cell lines remain *SMAD4* proficient. Using immunofluorescent staining, it has confirmed the efficiency of *SMAD4* knockdown in Huh7, Huh6 and PLC cell lines (Figure 3b).

Colony formation assay is a robust tool to evaluate the ability of a single cell to support proliferation. Using this assay, we observed a significant decrease in the numbers of formed colonies in Huh7 cells with *SMAD4* knockdown compared with the mock cells (CTR vs sh-*SMAD4*:  $270.8 \pm 25.82$  vs  $144.8 \pm 32.11$  colonies per 1000 cells, mean  $\pm$  s.d.,  $n = 4$ ,  $P < 0.05$ ) (Figure 3c). Similar results were observed in Huh6 and PLC cells (Figure 3c). Thus, in contrast to most other cell types where *SMAD4* expression is associated with reduced cancer cell growth, *SMAD4* expression supports proliferation of HCC cells.

Knockdown of *SMAD4* attenuated the ability of HCC cell migration

Cell migration is a fundamental function underlying cellular processes including invasion or metastasis of cancer cells. We thus investigated the role of *SMAD4* in migration of HCC cells using a ring-barrier system (Figure 4a). Silencing of *SMAD4* expression resulted in attenuated migratory capacity toward the cell-free area in Huh7 cells. In Huh7 cells with *SMAD4* knockdown, quantification revealed a significant reduction in total migration (CTR vs sh-*SMAD4*:  $174.1 \pm 54.3 \mu\text{m}$  vs  $128.7 \pm 42.1 \mu\text{m}$ , mean  $\pm$  s.d.,  $n = 30$ ,  $P < 0.01$ ), effective migration (CTR vs sh-*SMAD4*:  $109.1 \pm 33.2 \mu\text{m}$  vs  $55.4 \pm 22.4 \mu\text{m}$ , mean  $\pm$  s.d.,  $n = 30$ ,  $P < 0.001$ ), migration efficiency (CTR vs sh-*SMAD4*:  $63.60 \pm 9.60\%$  vs  $43.95 \pm 16.62\%$  mean  $\pm$  s.d.,  $n = 30$ ,  $P < 0.0001$ ) and migration velocity (CTR vs sh-*SMAD4*:  $7.3 \pm 2.3$  vs  $5.4 \pm 1.8 \mu\text{m/h}$ , mean  $\pm$  s.d.,  $n = 30$ ,  $P < 0.001$ ) (Figure 4b). These results indicate that *SMAD4* in HCC cells support migration and in conjunction with the colony formation data support the notion of a non-canonical pro-oncogenic function of *SMAD4* in HCC.

Silencing of *SMAD4* limited hepatoma initiation and growth in mice

To finally ensure the tumor-promoting effects of *SMAD4*, we evaluated the impact of *SMAD4* loss on tumor initiation and growth in nude mice. One million CTR and *SMAD4* knockdown cells were subcutaneously injected into the left or right side of the mice, respectively. As shown in Figure 5, impressively, knockdown of *SMAD4* in Huh7 cells resulted in complete abolishment of tumor formation, whereas 7 out of 10 mice in the CTR group formed tumor (weight:  $0.59 \pm 0.15$  g, mean  $\pm$  s.e.m.,  $n = 7$ ). Collectively, this result is in line with the outcomes of our *in vitro*

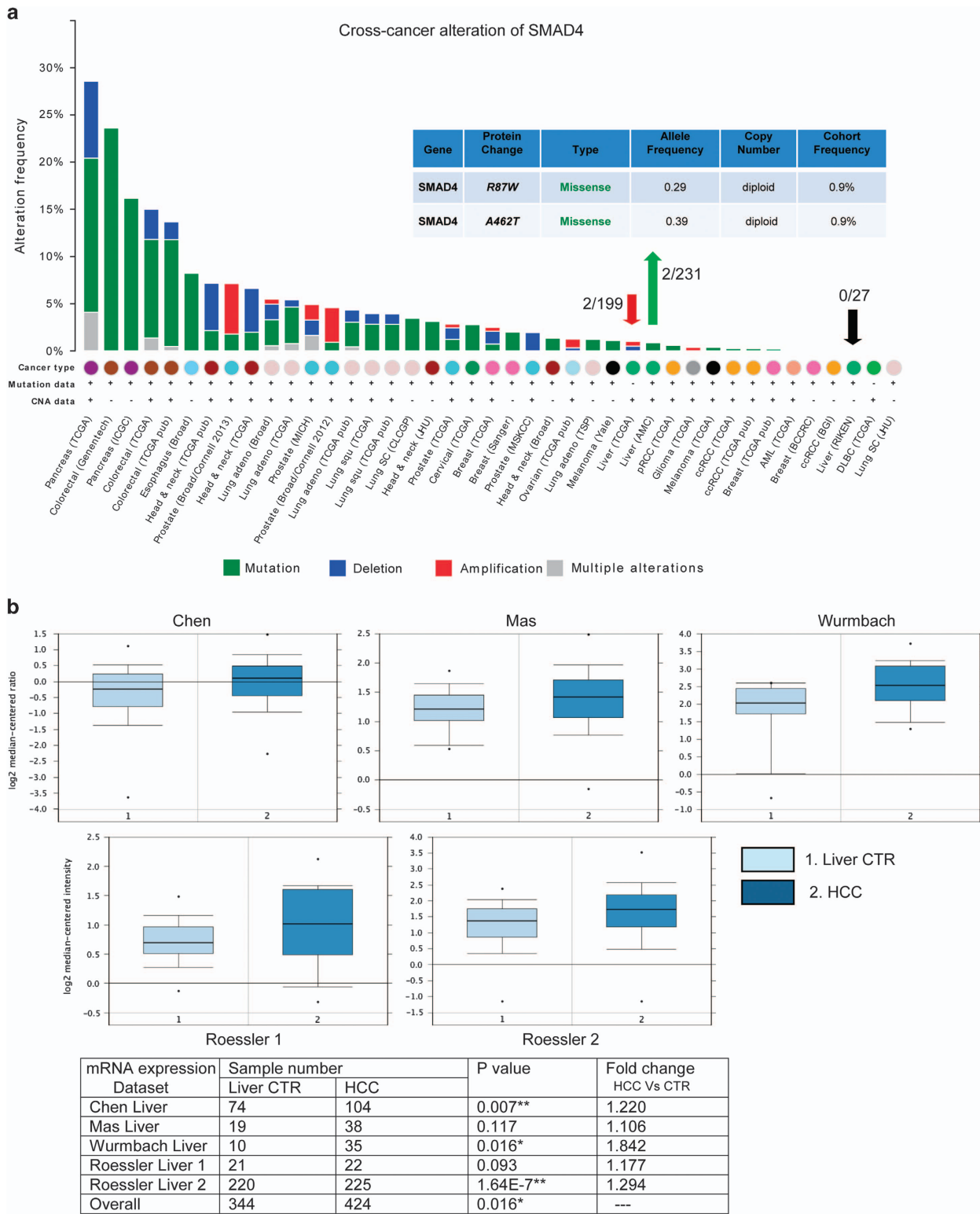


**Figure 1.** SMAD4 gene mutation is rare but upregulation of its mRNA expression is common in patient HCC. (a) In the database of the cBioPortal for Cancer Genomics (<http://www.cbioportal.org/public-portal/>), three cohorts of total 457 HCC patients with genomics data of SMAD4 gene were identified. There are only two HCC patients harboring mutations (R87W; A462T). In addition, one HCC patient has SMAD4 gene amplification and another one has SMAD4 deletion. Green arrow indicated the cohort identified SMAD4 mutation (2 of 231 HCC patients); red arrow indicated the cohort identified SMAD4 copy number variation (2 of 199 patients); and dark arrow indicated the cohort without genomic alteration identified (27 patients). (b) The Oncomine microarray database (<https://www.oncomine.org>) was searched to analyze mRNA expression of SMAD4 in patient HCC. In total, five cohorts of 424 HCC tissue samples compared with 344 liver tissues were identified. SMAD4 mRNA was upregulated in all the cohorts. There is a statistically significant increase of SMAD4 mRNA expression in the HCC tumor compared with liver tissue by polling all the cohorts. T-test was used for individual cohort. Meta-analysis of the five cohorts indicated its P-value for the median-ranked analysis. \* $P < 0.05$ , \*\* $P < 0.01$ .



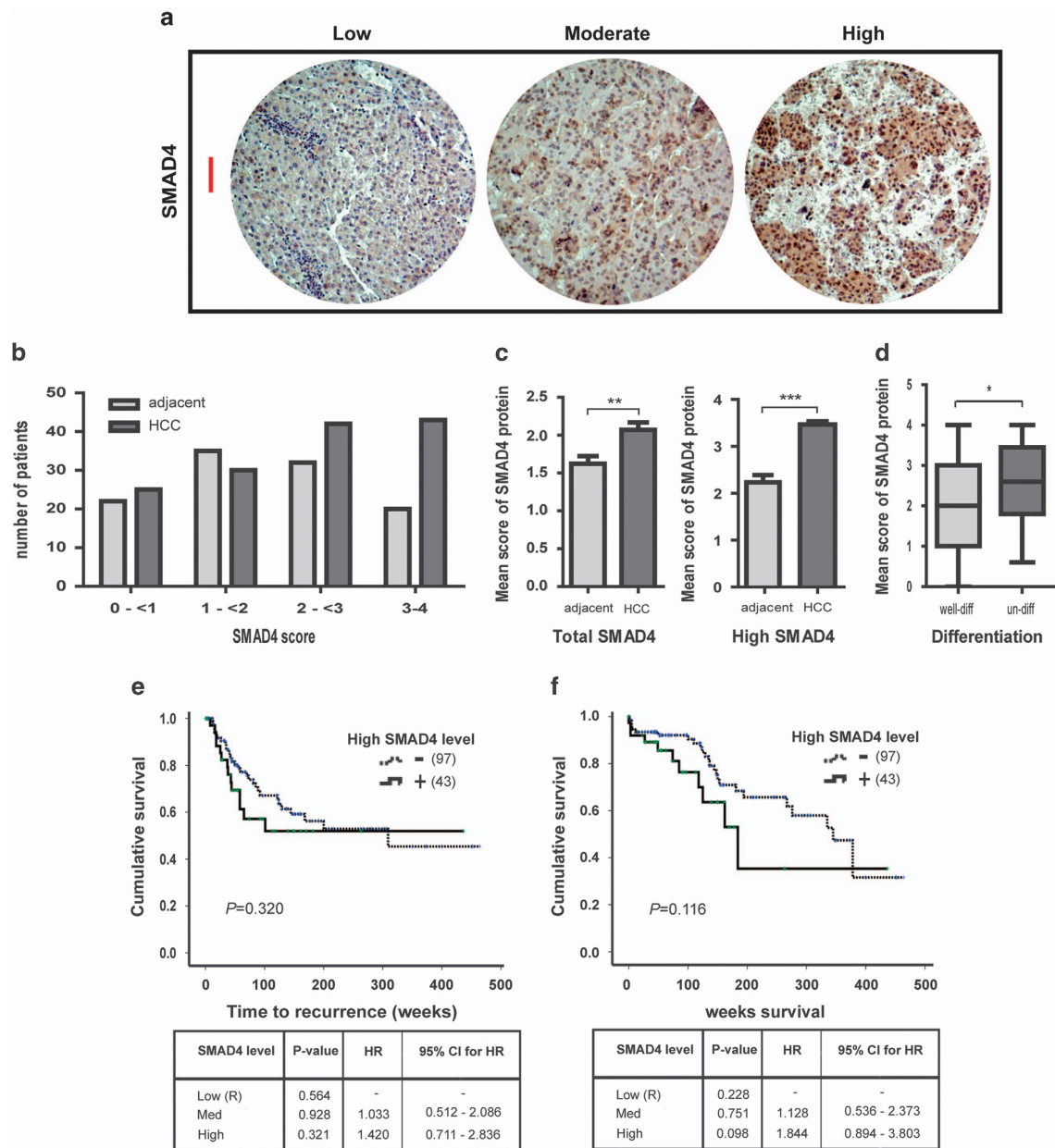


**Figure 2.** Strong elevation of nuclear SMAD4 expression in the tumors of sub-population of HCC patients. **(a)** The levels of SMAD4 protein positivity range from low (score: 0–<2), moderate (score: 2–<3) to high (score: 3–4) both in the HCC tumors and their adjacent sites. Scale bar, 100 pixels. **(b)** The distribution of SMAD4 score among HCC patients. **(c)** Overall, SMAD4 expression levels were significantly higher in human HCC tissues compared with normal adjacent liver tissues. Error bars represents mean  $\pm$  s.e.m. from  $n = 140$ , paired  $t$ -test,  $^{**}P < 0.01$ . A significant increase was also observed in tumors compared with adjacent tissues in the high-grade patients ( $n = 43$ , paired  $t$ -test,  $^{***}P < 0.001$ ). **(d)** Nuclear SMAD4 level was significantly higher in undifferentiated tumor than in well-differentiated tumor of HCC  $^{*}P < 0.05$ . From Cox regression analysis ( $n = 130$  analyzable patients), high SMAD4 level in surgical resected HCC tumor tend to have higher risk of fast recurrence (HR = 1.420) **(e)** and higher risk of poor survival (HR = 1.844) **(f)**. Kaplan–Meier analysis ( $n = 130$ ) also indicated a trend of faster disease recurrence **(e)** and lower cumulative survival **(f)**, although not statistically significant.

experimentation and the observation that high SMAD4 expression in human HCC tissue is associated with worse prognoses firmly demonstrates that SMAD4 exerts a tumor-promoting role in HCC.

Simultaneous elevation of SMAD4 and phosphorylated SMAD2/3 is significantly associated with poor patient outcome  
Upon binding of the cognate ligands to the TGF $\beta$  receptor, phosphorylated SMAD2/3 (p-SMAD2/3) binds to SMAD4 to form

heteromeric complex, translocate to the nucleus and activate TGF $\beta$  signaling.<sup>16</sup> The signaling receptors phosphorylate R-SMAD proteins at the carboxy-terminal (C-terminal) and the linker region.<sup>17</sup> Recent studies uncover a role for agonist-induced phosphorylation of the R-SMAD linker region<sup>18</sup> that may modulate downstream cellular responses to the TGF $\beta$  family of ligands. We thus performed immunohistochemistry staining of p-SMAD2/3 both at the C-terminal phosphorylation (p-SMAD2/3C, Ser423/425) and the linker phosphorylation region (p-SMAD2/3L, Thr220/179) in the tissue microarray (TMA) that was used for SMAD4 staining



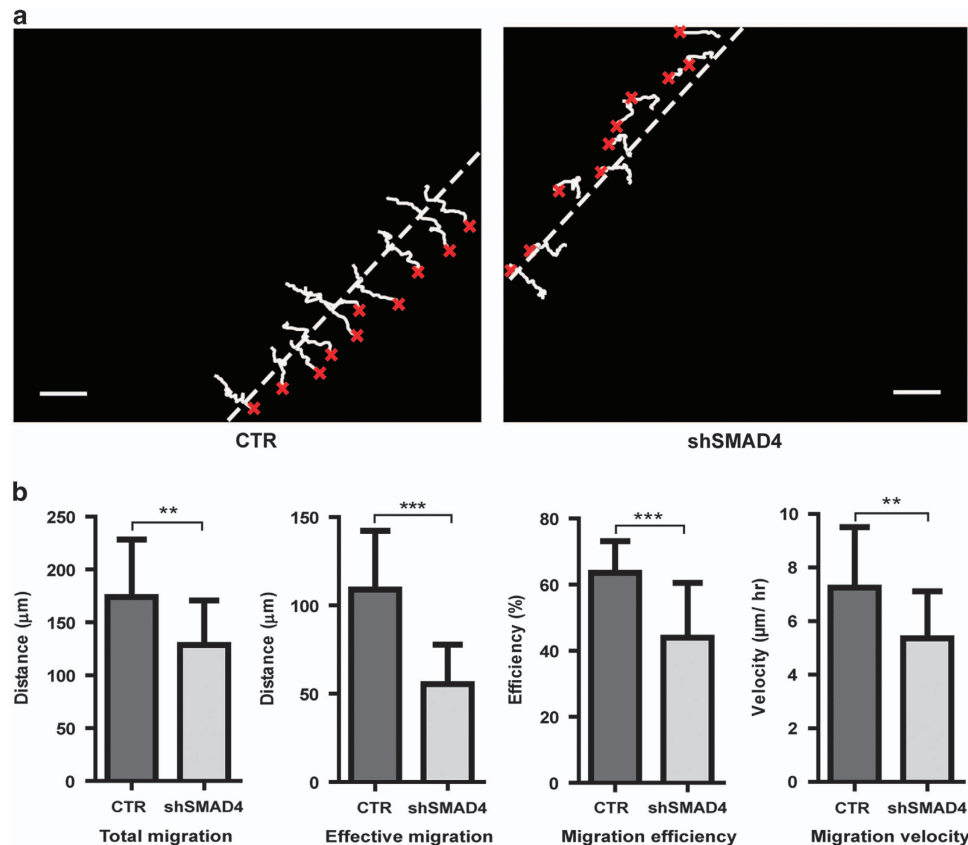


**Figure 4.** Silencing of SMAD4 inhibited HCC cell migration. (a) Migration assay of Huh7 cells (CTR) and its sh-SMAD4 cells using ring-barrier method system. (b) Quantification revealed a significant reduce in total migration, effective migration, migration efficiency and migration velocity in 24 h in SMAD4 knockdown cells compared with the control cells. Error bars represent mean  $\pm$  s.d. from  $n = 30$ , Mann-Whitney test, \*\* $P < 0.01$ , \*\*\* $P < 0.001$ , NS, not significant. Scale bar, 100  $\mu\text{m}$ .

( $n = 140$ ). The levels of p-SMAD2/3-C/L protein positivity range from low (score: 0–<2), moderate (score: 2–<3) to high (score: 3–4) both in the HCC tumors and their adjacent sites (Figures 6a and 7a). The patient groups (low, moderate or high) is categorized according to expression levels in the tumors. Although no significant difference overall ( $n = 140$ ), p-SMAD2/3C levels were significantly lower in HCC tissue as compared with normal adjacent liver tissue in patients with low-to-moderate scores ( $n = 86$ ,  $P < 0.001$ , data not shown); whereas it is significantly higher in the tumor of in patients with high scores ( $n = 54$ ,  $P < 0.001$ ) (Figure 6b). Moreover, overall p-SMAD2/3L expression was significantly higher in the HCC tumor than in the adjacent area ( $P < 0.001$ ) (Figure 7b). High p-SMAD2/3C expression in tumor is significantly associated with high recurrence rate ( $n = 47$ ,  $P < 0.05$ ) and patient death rate ( $n = 44$ ,  $P < 0.05$ ) (Supplementary Table 2). Cox regression and Kaplan–Meier analysis ( $n = 140$ ) also revealed a tendency of shorter time to recurrence and a trend to less cumulative survival in patients with high levels of p-SMAD2/3-C/L in the tumor HCC (Figures 6c and d and 7c).

As a phosphorylated protein, moderate levels of p-SMAD2/3-C/L would be expected to be already sufficient to trigger the downstream signaling transduction in the presence of SMAD4. A sub-population of HCC patients have a simultaneous elevation of SMAD4 and p-SMAD2/3C ( $n = 22$ ) and p-SMAD2/3L ( $n = 34$ ), which represents as a hallmark for the activation of the downstream signaling of TGF $\beta$  (Supplementary Figure S3 and S4; Figures 6f and 7c). Cox regression and Kaplan–Meier analysis also confirmed that these patients are significantly faster

to disease recurrence and worse survival ( $P < 0.05$ ) (Figures 6f and 7c).

Nuclear p-SMAD3L (Ser213) binds to SMAD-binding element in the promoter with high affinity and specificity<sup>19</sup> and transmits fibrogenic/carcinogenic (fibro-carcinogenic) signaling.<sup>20</sup> Both pSMAD3C(Ser425) and p-SMAD3L(Ser213) form hetero-complexes with SMAD4, and move to nucleus.<sup>21</sup> Chronic inflammation and hepatitis viral additively shift hepatocytic SMAD3 signaling from tumor-suppressive pSMAD3C to fibro-carcinogenic p-SMAD3L.<sup>22,23</sup> Therefore, we also investigated the expression of this particular form in our cohort. p-SMAD3L levels were significantly higher in HCC tissue as compared with normal adjacent liver tissue. ( $P < 0.001$ , Figure 7e). Cox regression analysis and Kaplan–Meier analysis ( $n = 131$ ) indicated that patients with high level of p-SMAD3L have worse survival (HR=1.155, 95% CI: 1.117–5.371 in the high-level group) and these features were also seen in co-expression of SMAD4 and p-SMAD3L (Figure 7f). Taken together (Figures 6 and 7; Supplementary Tables S2–S7), these results indicate that SMAD4 together with p-SMAD2/3, both C-terminal (C) and linker phosphorylation (L), with Ser or Thr residues, exert a tumor-promoting function in HCC patients.

An antitumor signaling mediated by phosphorylated SMAD1/5/8 and SMAD4 is inactivated in majority of HCC patients. Upon binding of BMP ligands, phosphorylated SMAD1/5/8 (p-SMAD1/5/8) binds to SMAD4 to form heteromeric complex, translocate to the nucleus and activate BMP signaling.<sup>16</sup> Although



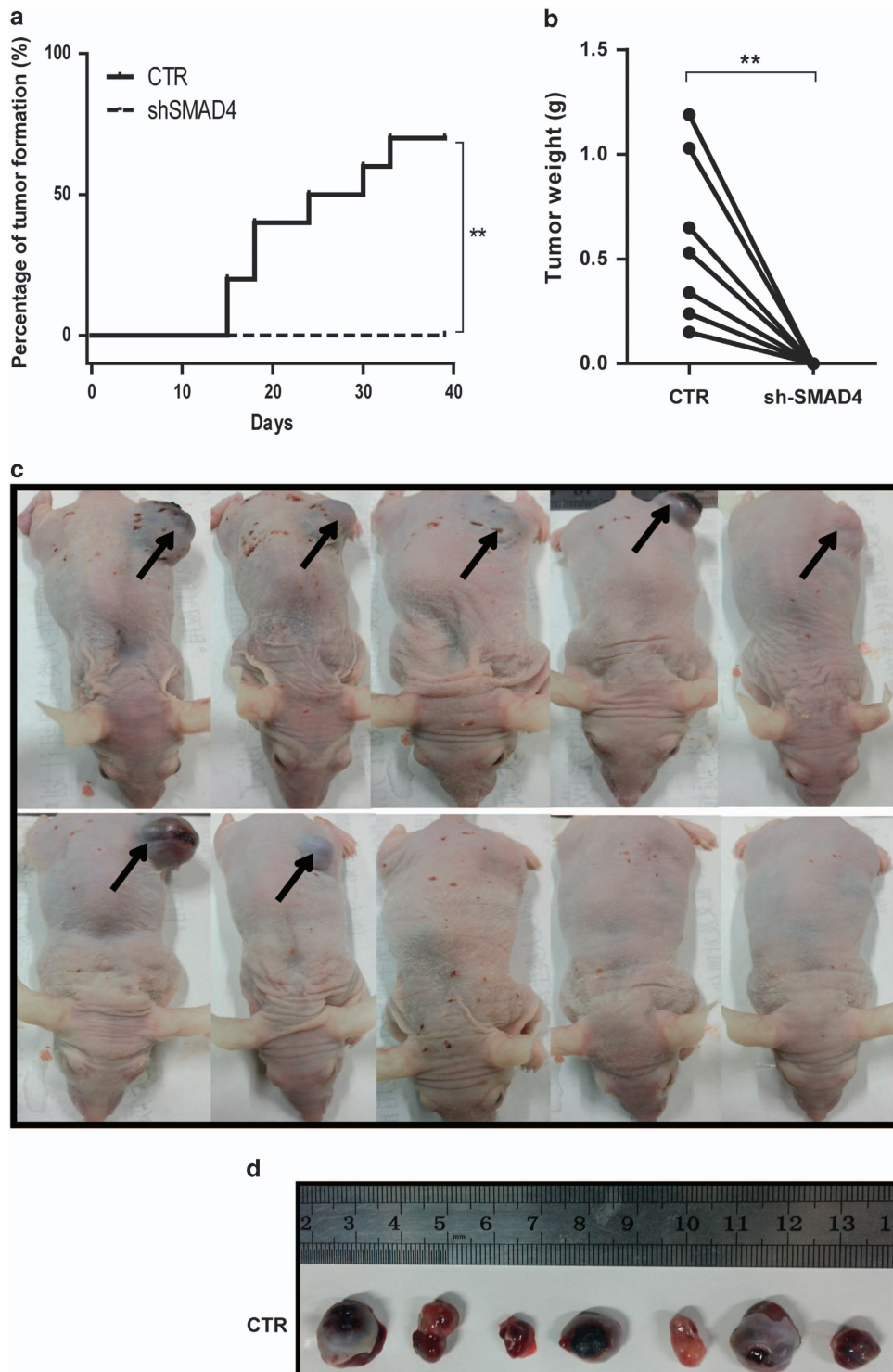


**Figure 5.** Knockdown of SMAD4 in Huh7 cells failed to initiate tumor in nude mice. **(a)** Knockdown of SMAD4 in Huh7 significantly abolished the tumor formation, whereas 7 out of 10 mice in the control group formed tumors (paired *t*-test,  $**P < 0.01$ ). **(b)** The weight of formed tumor. **(c)** The solid arrows indicate Huh7 in control group formed tumors in mice. **(d)** The appearance of formed tumors in centimeter length.

the exact role of BMP signaling in cancer is highly context dependent, a recent study demonstrated that BMP4, a BMP ligand, inhibited the tumorigenic capacity of HCC cells.<sup>24</sup> We further examined the effects of BMP4 on HCC cells. In Huh7 cells, BMP4 significantly reduces colony formation ability of Huh7 cells and

knockdown of SMAD4 attenuated the effects of BMP4. The efficiency of colony formation was reduced by BMP4 treatment in CTR cells by  $47.02 \pm 6.5\%$  but only by  $25.3 \pm 6.4\%$  in SMAD4 knockdown Huh7 cells (mean  $\pm$  s.d.,  $n = 4$ ,  $P < 0.01$ ) (Figure 8a). Consistently, adding BMP inhibitor Noggin appears to increase the



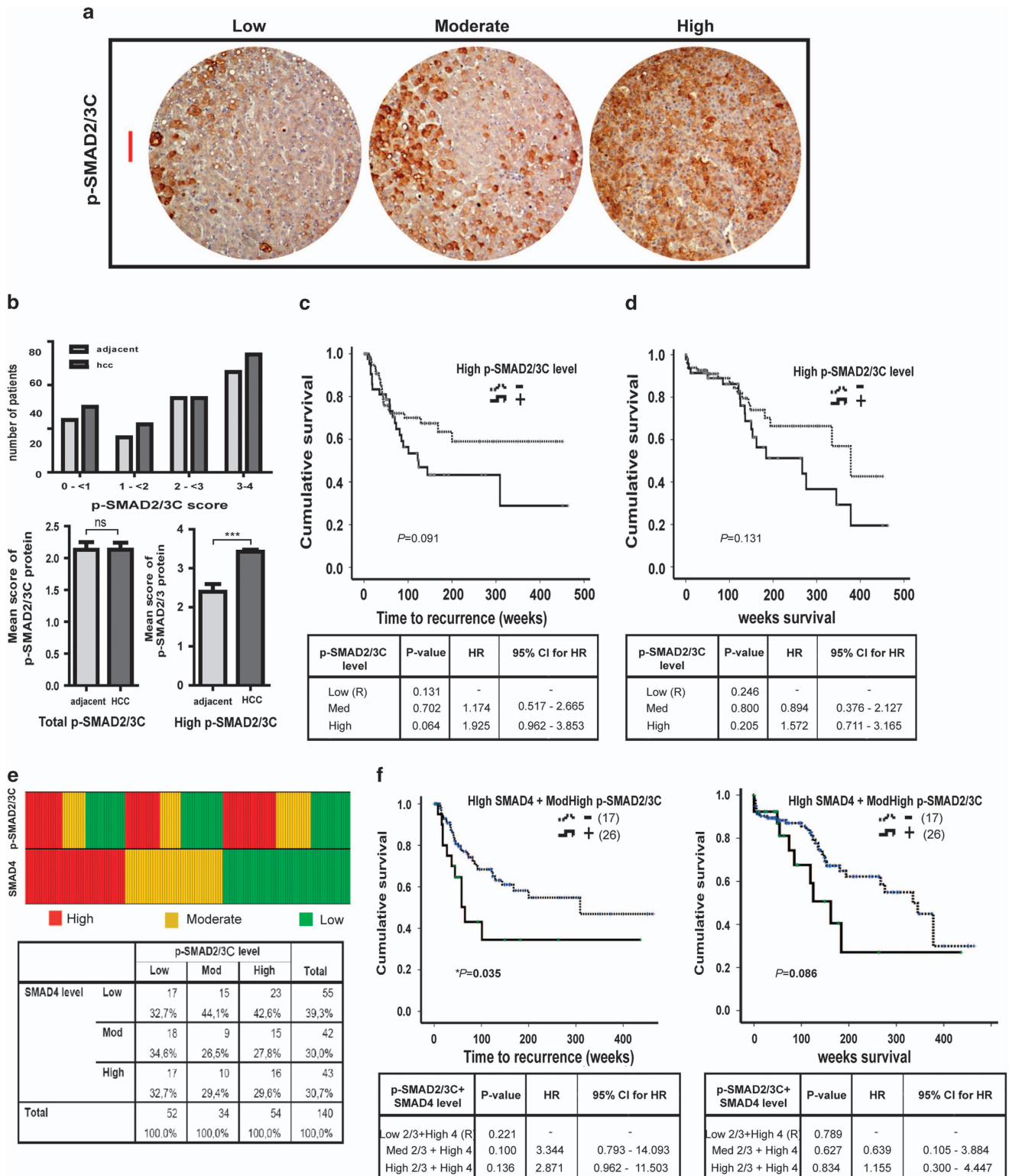


**Figure 6.** Simultaneous elevation of p-SMAD2/3C and SMAD4 is significantly associated with poor clinical outcome in HCC patients. **(a)** The levels of p-SMAD2/3C protein positivity range from low (score: 0–<2), moderate (score: 2–<3) to high (score: 3–4) both in the HCC tumors and their adjacent sites. Scale bar, 100 pixels. **(b)** There were more patients with higher p-SMAD2/3C score both in tumor and adjacent sites. No significant overall difference of p-SMAD2/3C expression between HCC tissue and normal adjacent liver tissue. Nevertheless, in the high-grade patients group, p-SMAD2/3C expression was significantly higher in HCC tissues compared with adjacent sites ( $n=54$ ). Error bars represents mean  $\pm$  s.e.m., paired  $t$ -test, \*\*\* $P < 0.001$ . From Cox regression and Kaplan–Meier analysis ( $n=130$ ), high levels of p-SMAD2/3C tend to have higher risk of fast recurrence (HR = 1.649) **(c)** and tend to have higher risk of poor survival (HR = 1.633) **(d)**. **(e)** Twenty-two out of 140 patients have simultaneously sufficient levels of both p-SMAD2/3C ( $n=16$  high;  $n=6$  moderate levels) and SMAD4. **(f)** These patients have significantly poor clinical outcome as shown by both Cox regression and Kaplan–Meier analysis. \* $P < 0.05$ . NS, not significant.

efficiency of colony formation in CTR cells ( $124.5 \pm 19.1\%$ , mean  $\pm$  s.d.,  $n=4$ ) but has much less effect ( $109.6 \pm 9.5\%$ , mean  $\pm$  s.d.,  $n=4$ ) in SMAD4 knockdown Huh7 cells (Figure 8b). Thus, BMP4 significantly reduced the colony formation ability of hepatoma cells, which was consistent with previous reports in other cancer,<sup>25–27</sup> and knockdown of SMAD4 attenuated the effects of BMP4. Western blot analysis showed the effects of BMP4 and Noggin on the protein levels of SMAD4, p-SMAD2/3 and p-SMAD1/5/8. This was in broad agreement with the efficacy of the experimental strategy but also suggested the existence of SMAD4-dependent feedback loops on BMP signaling elements (Figures 8c and d). Our results confirm that activation of BMP signaling, which involves both SMAD4 and p-SMAD1/5/8, exerts anti-HCC effects.

Next, we further explored the role of this pathway in our HCC cohort. Immunohistochemistry staining of p-SMAD1/5/8 was performed in the TMA ( $n=140$ ), and was scored and categorized as described before (Figures 9a and b). Although p-SMAD1/5/8 is significantly higher in the tumor tissue compared with adjacent liver tissue (Figure 9c), only a small subset of patients have high levels of p-SMAD1/5/8 in the tumor (17 out of 140, see Supplementary Table S8). No significant relation was observed regarding to the size ( $n=98$ ) and the number of tumor foci ( $n=129$ ) (Supplementary Table S8). Interestingly, a Bonferroni-corrected clinical parameter analysis revealed a negative correlation between tumor p-SMAD1/5/8 level and age (Supplementary Table S8). Patients with high levels of p-SMAD1/5/8 appear to have lower risk of fast recurrence (HR=0.542, 95% CI: 0.191–1.538 in the high-level group) and lower risk to poor survival (HR=0.596, 95% CI: 0.210–1.697 in the high-level group) (Figure 9d). Kaplan–Meier analysis also revealed a trend of longer time to recurrence and higher cumulative survival in these patients (Figure 9d).

As a phosphorylated protein, p-SMAD1/5/8 could sensitively control the downstream signaling transduction. As the anti-tumor function of this signaling requires both SMAD4 and p-SMAD1/5/8, we further categorized the expression levels of both proteins in the same patients. As shown in Figure 9e, there are only eight patients having simultaneously sufficient levels of both SMAD4 and p-SMAD1/5/8 ( $n=2$  high;  $n=6$  moderate levels). These results suggest that SMAD4 and p-SMAD1/5/8-mediated antitumor signaling is inactivated in majority of our HCC patients.

## DISCUSSION

In this study, we reported a drastic elevation of nuclear SMAD4 localization in tumors of subset of HCC patients. High expression of SMAD4 was further demonstrated to be functionally important for hepatoma formation and progression. Importantly, simultaneous elevation of SMAD4 and p-SMAD2/3 in sub-population of HCC patients significantly associated with poor outcome after surgery. Although SMAD4 coupled with p-SMAD1/5/8 can also mediate an antitumor effect, this signaling, however, is silent in majority of our HCC patients. Thus, we conclude that high nuclear SMAD4 expression has been screwed toward a tumor-promoting signaling in HCC (Supplementary Figure S5). This is unexpected in view of the dogma that SMAD4 is a potent tumor suppressor.

SMAD4 was initially described in pancreatic cancer, named DPC4 (deleted in pancreatic carcinoma, locus 4), and appears critical in pancreatic cancer progression.<sup>28,29</sup> SMAD4 loss occurs in 40–50% of colon cancers,<sup>30</sup> which is associated with metastasis, advanced disease and reduced survival. Similarly, its loss in cholangiocarcinoma<sup>31</sup> or prostate cancer<sup>8</sup> is also related to more progressive disease. The tumor-suppressor function of SMAD4 is often closely linked to its capacity to mediate TGF $\beta$  and BMP signals. However, we question whether activation or silencing of

TGF $\beta$ /BMP downstream components, including SMADs, is always ligand dependent in cancer? As in xenografts of human hepatoma cell lines in mice, which are thus unlikely to encounter their (human) ligands, we observed that high expression of SMAD4 is even required for tumor formation and growth. In contrast to our observation, a previous study has reported a lower protein level of SMAD4 in HCC tissue compared with adjacent liver tissue in an Asian cohort.<sup>32</sup> A possible explanation could be that the etiologies of HCC may influence the expression of SMAD4. In Asia, viral hepatitis is the main cause of HCC; whereas only <30% of patients in our European cohort have viral hepatitis history, although high expression of SMAD4 was also reported in another Asian HCC cohort.<sup>33</sup> In addition, technical differences, including the source of antibody and the protocol of immunohistochemical staining, may also result in discrepancy. In this study, we have used a robust staining protocol for SMAD4 (see Materials and methods section) that was optimized and established in our previous studies.<sup>34,35</sup>

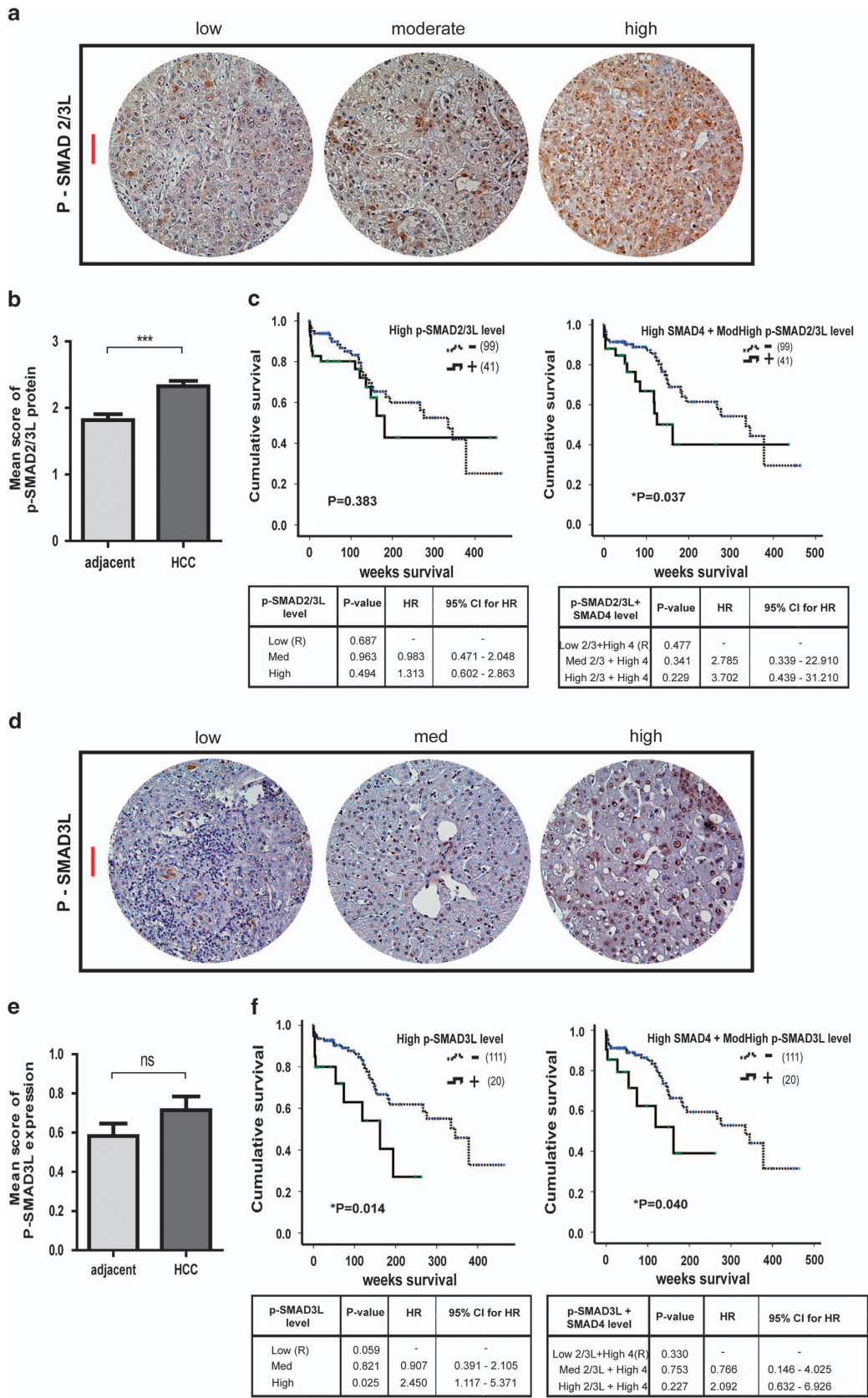
The essential role of TGF $\beta$ /BMP signaling in cancer is certainly well documented, whereas its exact functions are also context dependent.<sup>36</sup> TGF $\beta$ 1 was also well recognized for its dual role in carcinogenesis.<sup>37</sup> It acts as a tumor suppressor in early stages of hepatocarcinogenesis by inducing apoptosis<sup>38</sup> and at a later stage, however, liver tumor cells often become resistant to its pro-apoptotic effect, and produce large amounts of TGF $\beta$  themselves.<sup>39</sup> This was in line with our result that the different levels of phosphorylated R-SMADs is associated with distinct patient outcome. We speculate that dysregulation of key R-SMADs may lead to the opposite effect of the canonical TGF $\beta$  and BMP signaling. In our HCC cohort, a sub-population of HCC patients have a simultaneous elevation of SMAD4 and p-SMAD2/3C ( $n=22$ ) or p-SMAD2/3L ( $n=34$ ), indicating the activation of TGF $\beta$  downstream signaling. Both high expression of the C-terminal (C) and linker phosphorylation (L) region of p-SMAD2/3 are associated with worse outcome after surgical resection in our HCC cohort, which is in line with previous report in colorectal cancer,<sup>40</sup> confirming a tumor-promoting function of TGF $\beta$  signaling in these HCC patients.

Several distinct BMP ligands were reported to act together to promote the migratory and invasive potential of cancer cells,<sup>41</sup> including in HCC.<sup>42,43</sup> In contrast, a recent study demonstrated that BMP4 induced differentiation of HCC cancer stem cells and inhibited their tumorigenic capacity.<sup>24</sup> Our *in vitro* study indicated activating BMP signaling by adding BMP4 ligand in HCC was able to effectively suppress colony formation of HCC cells, which was consistent with previous reports in other cancer.<sup>25–27</sup> However, silencing of SMAD4 gene attenuated this effect, confirming that these anti-oncogenic actions require basal levels of SMAD4. Despite an antitumor effects of BMP pathway, this signaling, however, is silent in majority of our HCC patients, by losing the key components, either SMAD4 or p-SMAD1/5/8, or both of them. The obvious implication of this observation is that HCC cells should prove exquisitely sensitive to stimulation with BMP ligands mediating such signaling. In conjunction with the recent Food and Drug Administration approval of BMP2 and BMP7 as treatment for certain bone pathologies.<sup>44</sup> However, we have to be cautious that there are also studies reporting pro-oncogenic roles of BMP ligands in particular settings. For instance, BMP7 and BMP9 have been shown to have tumor-promoting functions in some experimental cancer (including HCC) models.<sup>42,45,46</sup> Nevertheless, our results call for further study exploiting this Achilles' heel of HCC.

In summary, this study reports a significant elevation of nuclear SMAD4 localization in patient HCC tumors. High nuclear SMAD4 has been screwed toward tumor-promoting effects because of simultaneous elevation of p-SMAD2/3 in subset of patients. SMAD4 can also mediate an antitumor signaling by coupling

p-SMAD1/5/8; this complex, however, is absent in majority of patients because of lack of either SMAD4 or p-SMAD1/5/8, or both of them. These results have certainly shed new light on the

molecular biology of HCC and more importantly SMAD-based molecules may have potential as outcome predictors for patient stratification.





## MATERIALS AND METHODS

### Tissue microarray

To make TMA, paraffin-embedded HCC patient tissues ( $n = 140$ , between 2004 and 2013) were collected from the Pathology Department of Erasmus Medical Centre (Erasmus MC) Rotterdam. The use of patient materials was approved by the medical ethical committee of Erasmus MC (Medisch Ethische Toetsings Commissie Erasmus MC).<sup>47,48</sup>

### Bioinformatics analysis of genomics and mRNA assay data sets

To analyze the prevalence of genomic alterations of *SMAD4* gene in patient HCC tissues, the database of the cBioPortal for Cancer Genomics (<http://www.cbioportal.org/public-portal/>) was searched. Both copy number variation and gene mutation data were analyzed across cancer types with focusing on HCC.

To analyze mRNA expression of *SMAD4* in HCC, the Oncomine microarray database (<https://www.oncomine.org>) was searched. *SMAD4* mRNA expression was analyzed in identified cohorts by comparing expression levels in HCC tumors with liver tissues.

### Immunohistochemistry

Paraffin-embedded liver tumor tissue in TMA slides were deparaffinized in xylene, rehydrated in graded alcohols. For antigen retrieval, slides were boiled in Tris/EDTA pH 9.0 for 30 min (for *SMAD4* antibody) and 10 min for other antibodies; 3%  $H_2O_2$  was used to block endogenous peroxidase for 10 min at room temperature. The slides were incubated in 5% milk blocking solution followed by overnight incubation in mouse *SMAD4* antibody (1:100 dilution, Santa Cruz Biotechnology, Inc., Huissen, The Netherlands), goat p-*SMAD2/3C* (Ser423/425) antibody (1:250 dilution, Santa Cruz Biotechnology, Inc.), mouse p-*SMAD2/3L* (Thr220/179) (1:250 dilution, Takara Bio, Shiga, Japan), mouse p-*SMAD3L* (Ser213) (1:250 dilution, Takara Bio), rabbit p-*SMAD1/5/8* (1:500 dilution, Cell Signaling, Leiden, The Netherlands) and p-Histone H3 (1:1000 dilution, Merck Millipore, Amsterdam, The Netherlands), and then counterstained with hematoxylin. The *SMAD4* scoring was based on the nuclear staining and the p-*SMAD2/3* and p-*SMAD1/5/8* scoring were based on cytoplasm and/or nuclear staining. The following scores were applied: score 0 for 0–10% positive staining, score 1 for 10–30% positive staining, score 2 for 30–70% positive staining, score 3 for >70% positive staining and

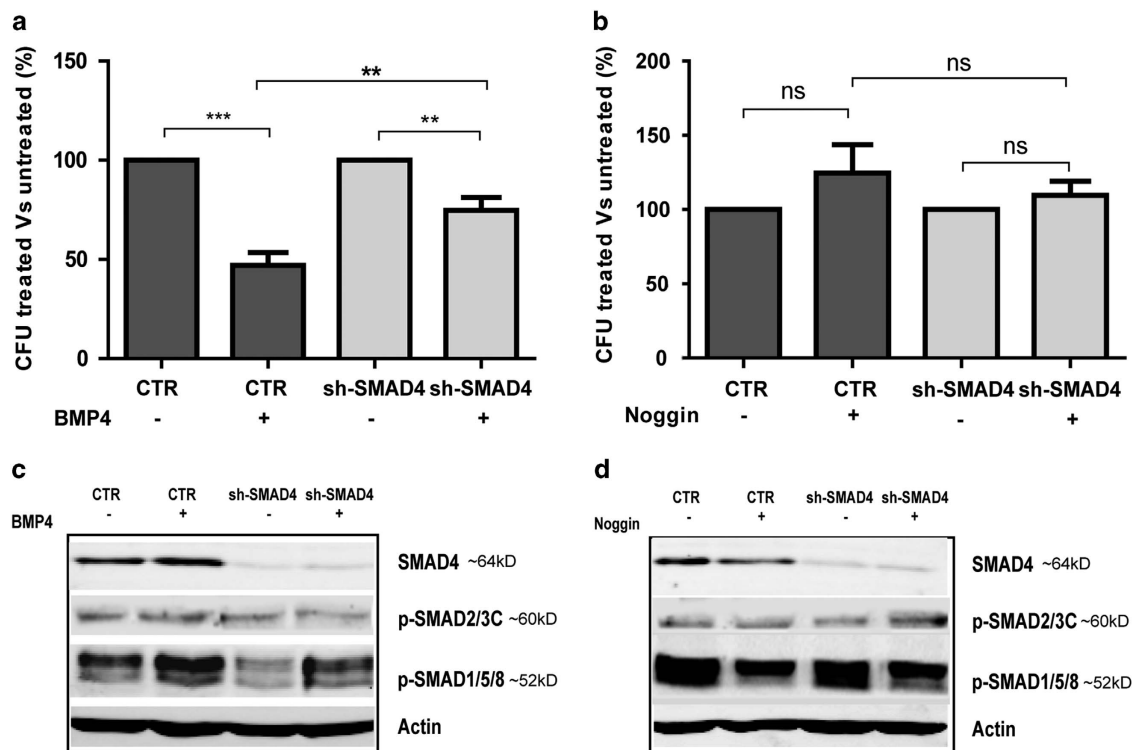


**Figure 8.** BMP4 significantly reduced the colony formation ability of HCC cells and its ability was attenuated by silencing *SMAD4*. **(a)** The efficiency of decreasing colony formation by BMP4 treatment was significantly reduced in Huh7 cells with *SMAD4* knockdown. Error bars represent mean  $\pm$  s.d. from  $n = 4$ ,  $^{**}P < 0.01$ ,  $^{***}P < 0.001$ . **(b)** Although the difference was not statistically significant, adding BMP inhibitor Noggin appeared to increase the efficiency of colony formation in control cells and to a lesser extent in *SMAD4* knockdown Huh7 cells. Error bars represent mean  $\pm$  s.d. from  $n = 4$ , NS, not significant. **(c)** Protein levels of *SMAD4*, phospho-*SMAD2/3* and phospho-*SMAD1/5/8* after BMP4 treatment and **(d)** protein levels of *SMAD4*, phospho-*SMAD2/3* and phospho-*SMAD1/5/8* after Noggin treatment.

**Figure 7.** Simultaneous elevation of p-*SMAD2/3L* and *SMAD4* is significantly associated with poor clinical outcome in HCC patients. The levels of p-*SMAD2/3L* **(a)** and p-*SMAD3L* **(d)** protein range from low (score: 0–<2), moderate (score: 2–<3) to high (score: 3–4) both in the HCC tumors and their adjacent sites. Scale bar, 100 pixels. **(b)** P-*SMAD2/3L* expression was significantly higher in HCC tissues compared with adjacent sites. Error bars represents mean  $\pm$  s.e.m., paired *t*-test,  $^{***}P < 0.001$ . **(c)** High levels of p-*SMAD2/3L* tend to have higher risk of poor survival (HR = 1.313) and 34 out of 140 patients have simultaneously sufficient levels of both p-*SMAD2/3L* and *SMAD4*. These patients have significantly poor clinical outcome as shown by both Cox regression and Kaplan–Meier analysis,  $^{*}P < 0.05$ . **(e)** The p-*SMAD3L* expression had no difference in HCC tissues compared with adjacent sites. Error bars represents mean  $\pm$  s.e.m., paired *t*-test, NS, not significant. **(f)** High levels of p-*SMAD3L* tend to have higher risk of poor survival (HR = 2.450) and 21 out of 140 patients have simultaneously sufficient levels of both p-*SMAD3L* and *SMAD4*. These patients have significantly poor clinical outcome as shown by both Cox regression and Kaplan–Meier analysis.  $^{*}P < 0.05$ .



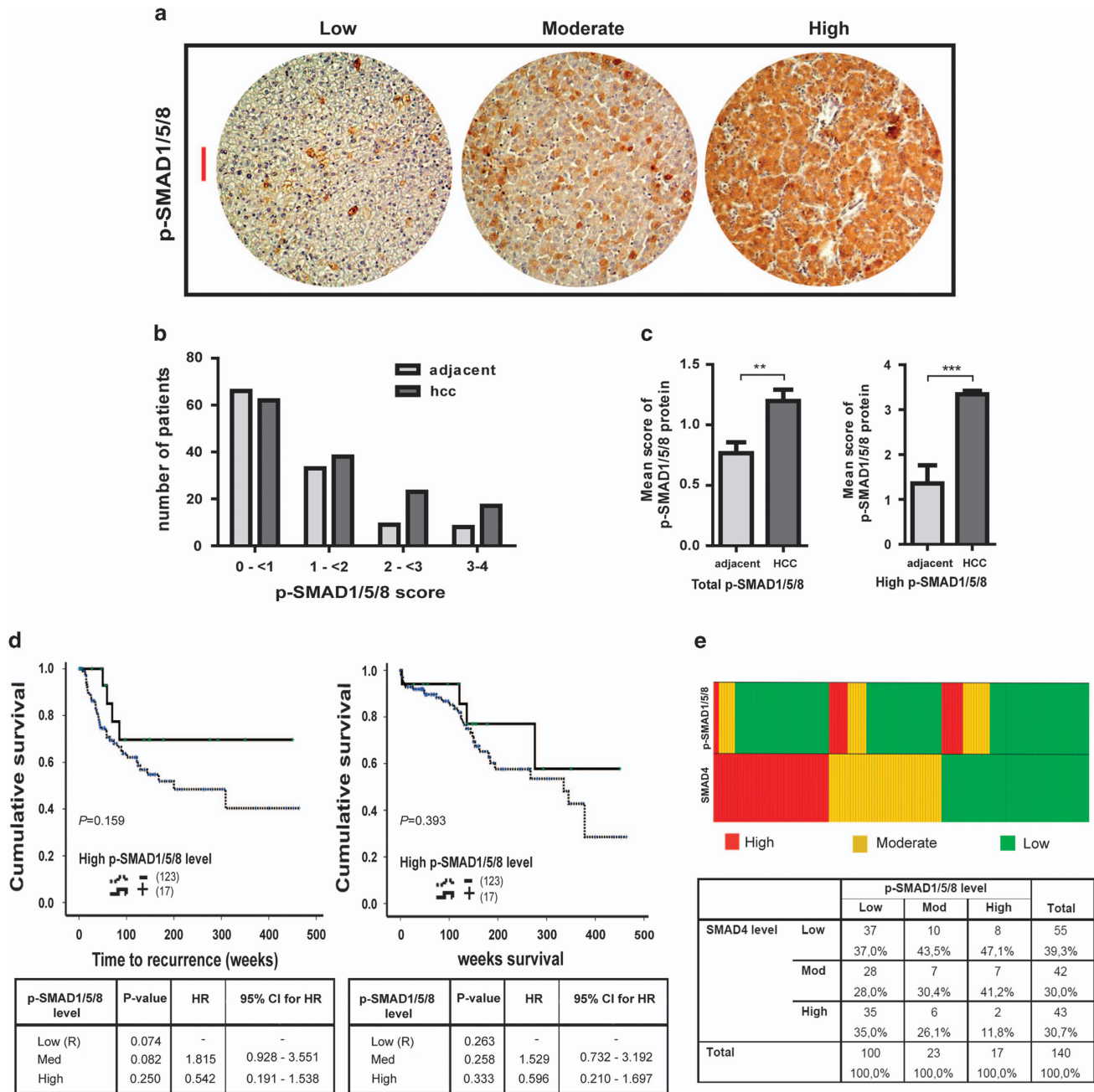


**Figure 9.** The antitumor signaling mediated by p-SMAD1/5/8 and SMAD is inactivated in most of the HCC patients. **(a)** The levels of p-SMAD1/5/8 protein positivity range from low (score: 0–<2), moderate (score: 2–<3) to high (score: 3–4) both in the HCC tumors and their adjacent sites. Scale bar, 100 pixels. **(b)** Different to SMAD4 or p-SMAD2/3, there were less patients with high p-SMAD1/5/8 score both in tumor and adjacent sites. **(c)** Overall p-SMAD1/5/8 expression was significantly higher in HCC tissue compared with adjacent liver tissue. The p-SMAD1/5/8 levels were also significantly higher in HCC tissue compared with adjacent tissue in the high-grade ( $n=17$ ) group. Error bars represents mean  $\pm$  s.e.m., paired  $t$ -test,  $**P < 0.01$ ,  $***P < 0.001$ . **(d)** From Cox regression analysis ( $n=130$ ), patients with high level of p-SMAD1/5/8 tend to have less risk of fast recurrence (HR = 0.542) and less risk to poor survival (HR = 0.596). Kaplan–Meier analysis ( $n=130$ ) showed similar trends. **(e)** However, there are only eight patients who have simultaneously sufficient levels of both SMAD4 and p-SMAD1/5/8 ( $n=2$  high;  $n=6$  moderate levels), suggesting that this signaling is inactivated in most of the HCC patients.

score 4 for >70% positive staining+high intensity. The scorings were done by two investigators and the difference of scoring was valued by Kappa test.

#### Lentiviral short hairpin RNA vectors

Lentiviral backbone vectors for SMAD4 knockdown and non-targeting control were obtained from the Erasmus Center for Biomics (the Sigma–Aldrich TRC library, Zwijndrecht, The Netherlands). A vectors expressing short hairpin RNA targeting green fluorescent protein (not expressed in

HCC cell lines) served as control (CTR). Lentiviral viral particles were generated as described previously.<sup>49</sup>

#### Cell culture and reagents

Human hepatoma cell lines (Huh7, Huh6 and PLC) were cultured in Dulbecco's modified Eagle's medium (Lonza, Breda, The Netherlands) supplemented with 10% fetal bovine serum (Sigma–Aldrich) and 1% penicillin/streptomycin (Gibco, Bleiswijk, The Netherlands). SMAD4 knock-down cells and control cells were generated by inoculation of lentiviral

vectors and subsequently selected and maintained in Dulbecco's modified Eagle's medium with 10% fetal bovine serum, 1% penicillin/streptomycin and 2 µg/ml puromycin (Sigma-Aldrich). Recombinant human BMP4 protein (100 µg/ml, Merck Millipore) and recombinant human Noggin (50 µg/ml, R&D System, Oxon, UK) were used to treat cells, respectively.

### Colony forming assay

Colony formation was performed in Huh7 cells as described previously.<sup>48</sup> After trypsinizing, 1000 cells were added to each well of a six-well plate and were cultured in Dulbecco's modified Eagle's medium as previously described. The colonies formed are counterstained with hematoxylin and eosin after 2 weeks.

### Western blotting

Subconfluent cells were lysed in Laemmli sample buffer containing 0.1 M dithiothreitol and incubated for 5 min at 96 °C. Immunoblotting was performed using fluorescent Odyssey immunoblotting (LI-COR Biosciences, Lincoln, NE, USA). Antibodies used were mouse SMAD4 antibody (1:500 dilution, Santa Cruz Biotechnology, Inc.), goat p-SMAD2/3 antibody (1:500 dilution, Santa Cruz Biotechnology, Inc.) and rabbit p-SMAD1/5/8 (1:500 dilution, Cell Signaling). Quantification was performed using Odyssey LI-COR software.

### Ring-barrier migration assay

Ring-barrier-based migration assays were performed as previously described.<sup>50,51</sup> Huh7 and its sh-SMAD4 cells,  $3 \times 10^5$  cells were seeded in the ring in Dulbecco's modified Eagle's medium+10% fetal bovine serum +1% penicillin/streptomycin. After 24 h, the migration barrier was removed and the cells were washed twice followed by the addition of fresh medium. All cell tracking measurements were conducted using AxioVision 4.9.1 (Carl Zeiss Microscopy, LLC, Thornwood, NY, USA). *P*-values were calculated using the two-tailed Mann-Whitney test. Track diagram images were processed in Adobe Illustrator CS6 (Adobe Systems Inc., San Jose, CA, USA).

### HCC xenograft tumor in nude mice

HCC xenograft tumor model in nude mice was established as previously described.<sup>52</sup> Ten mice for each cell line (Huh7), aged 6–8 weeks, were subcutaneously engrafted with 1 million control (CTR) and SMAD4 knockdown cells into the lower left or right flank, respectively. Tumor initiation in the mice was monitored. At the end of experiment, mice were killed and tumors were harvested and weighed. The use of animals was approved by the Animal Care and Ethics Committee at Hangzhou Normal University, Hangzhou, China.

### Statistical analysis

Statistical analysis was performed by using  $\chi^2$  test, nonparametric Mann-Whitney test, Cox regression analysis and Kaplan–Meier survival analysis in IBM SPSS Statistical (IBM Corporation, Armonk, NY, USA). *T*-test was also used using GraphPad InStat software (GraphPad Software Inc., San Diego, CA, USA). *P*-values < 0.05 were considered as statistically significant.

### CONFLICT OF INTEREST

The authors declare no conflict of interest.

### ACKNOWLEDGEMENTS

We thank the support from the Daniel den Hoed Foundation for a Centennial Award fellowship (to Q Pan), the Netherlands Organization for Scientific Research (NWO/ZonMw) for a VENI grant (no. 916-13-032) (to Q Pan), the Dutch Digestive Foundation (MLDS) for a career development grant (no. CDG 1304) (to Q Pan) and the European Association for the Study of the Liver (EASL) for a Sheila Sherlock Fellowship (to Q Pan). Support from the Science and Technology Department Commonwealth Technology Applied Research Project (no. 2012F82G2060018) of Zhejiang Province, China and the National Nature Science Foundation of China (No. 81272687) (to K Chen) is gratefully acknowledged. We thank Dr Ron Smits from Erasmus Medical Center Rotterdam for critical reading of the manuscript and thank Dr Jie Xu from the Animal Care at Hangzhou Normal University, Hangzhou, China for helping with the animal experiments.

### REFERENCES

- Wakefield LM, Hill CS. Beyond TGFbeta: roles of other TGFbeta superfamily members in cancer. *Nat Rev Cancer* 2013; **13**: 328–341.
- Hardwick JC, Kodach LL, Offerhaus GJ, van den Brink GR. Bone morphogenetic protein signalling in colorectal cancer. *Nat Rev Cancer* 2008; **8**: 806–812.
- Shi Y, Massague J. Mechanisms of TGF-beta signaling from cell membrane to the nucleus. *Cell* 2003; **113**: 685–700.
- Shi Y, Hata A, Lo RS, Massague J, Pavletich NP. A structural basis for mutational inactivation of the tumour suppressor Smad4. *Nature* 1997; **388**: 87–93.
- Lagna G, Hata A, Hemmati-Brivanlou A, Massague J. Partnership between DPC4 and SMAD proteins in TGF-beta signalling pathways. *Nature* 1996; **383**: 832–836.
- Hahn SA, Hoque AT, Moskaluk CA, da Costa LT, Schutte M, Rozenblum E *et al*. Homozygous deletion map at 18q21.1 in pancreatic cancer. *Cancer Res* 1996; **56**: 490–494.
- Xu X, Kobayashi S, Qiao W, Li C, Xiao C, Radaeva S *et al*. Induction of intrahepatic cholangiocellular carcinoma by liver-specific disruption of Smad4 and Pten in mice. *J Clin Invest* 2006; **116**: 1843–1852.
- Ding Z, Wu CJ, Chu GC, Xiao Y, Ho D, Zhang J *et al*. SMAD4-dependent barrier constrains prostate cancer growth and metastatic progression. *Nature* 2011; **470**: 269–273.
- Zhang B, Halder SK, Kashikar ND, Cho YJ, Datta A, Gorden DL *et al*. Antimetastatic role of Smad4 signaling in colorectal cancer. *Gastroenterology* 2010; **138**: 969–980 e961-963.
- Itatani Y, Kawada K, Fujishita T, Kakizaki F, Hirai H, Matsumoto T *et al*. Loss of SMAD4 from colorectal cancer cells promotes CCL15 expression to recruit CCR1+ myeloid cells and facilitate liver metastasis. *Gastroenterology* 2013; **145**: 1064–1075 e1011.
- Argani P, Shaukat A, Kaushal M, Wilentz RE, Su GH, Sohn TA *et al*. Differing rates of loss of DPC4 expression and of p53 overexpression among carcinomas of the proximal and distal bile ducts. *Cancer* 2001; **91**: 1332–1341.
- Caputo V, Cianetti L, Niceta M, Carta C, Ciolfi A, Bocchinfuso G *et al*. A restricted spectrum of mutations in the SMAD4 tumor-suppressor gene underlies Myhre syndrome. *Am J Hum Genet* 2012; **90**: 161–169.
- Korsse SE, Biermann K, Offerhaus GJ, Wagner A, Dekker E, Mathus-Vliegen EM *et al*. Identification of molecular alterations in gastrointestinal carcinomas and dysplastic hamartomas in Peutz-Jeghers syndrome. *Carcinogenesis* 2013; **34**: 1611–1619.
- Tangkijvanich P, Anukulkarnkul N, Suwangool P, Lertmaharit S, Hanvivatvong O, Kullavanijaya P *et al*. Clinical characteristics and prognosis of hepatocellular carcinoma: analysis based on serum alpha-fetoprotein levels. *J Clin Gastroenterol* 2000; **31**: 302–308.
- Kocabayoglu P, Friedman SL. Cellular basis of hepatic fibrosis and its role in inflammation and cancer. *Front Biosci (Schol Ed)* 2013; **5**: 217–230.
- Ikushima H, Miyazono K. TGFbeta signalling: a complex web in cancer progression. *Nat Rev Cancer* 2010; **10**: 415–424.
- Massague J. TGFbeta signalling in context. *Nat Rev Mol Cell Biol* 2012; **13**: 616–630.
- Matsuzaki K. Smad phospho-isoforms direct context-dependent TGF-beta signaling. *Cytokine Growth Factor Rev* 2013; **24**: 385–399.
- Furukawa F, Matsuzaki K, Mori S, Tahashi Y, Yoshida K, Sugano Y *et al*. p38 MAPK mediates fibrogenic signal through Smad3 phosphorylation in rat myofibroblasts. *Hepatology* 2003; **38**: 879–889.
- Sekimoto G, Matsuzaki K, Yoshida K, Mori S, Murata M, Seki T *et al*. Reversible Smad-dependent signaling between tumor suppression and oncogenesis. *Cancer Res* 2007; **67**: 5090–5096.
- Mori S, Matsuzaki K, Yoshida K, Furukawa F, Tahashi Y, Yamagata H *et al*. TGF-beta and HGF transmit the signals through JNK-dependent Smad2/3 phosphorylation at the linker regions. *Oncogene* 2004; **23**: 7416–7429.
- Matsuzaki K, Murata M, Yoshida K, Sekimoto G, Uemura Y, Sakaida N *et al*. Chronic inflammation associated with hepatitis C virus infection perturbs hepatic transforming growth factor beta signaling, promoting cirrhosis and hepatocellular carcinoma. *Hepatology* 2007; **46**: 48–57.
- Murata M, Matsuzaki K, Yoshida K, Sekimoto G, Tahashi Y, Mori S *et al*. Hepatitis B virus X protein shifts human hepatic transforming growth factor (TGF)-beta signaling from tumor suppression to oncogenesis in early chronic hepatitis B. *Hepatology* 2009; **49**: 1203–1217.
- Zhang L, Sun H, Zhao F, Lu P, Ge C, Li H *et al*. BMP4 administration induces differentiation of CD133+ hepatic cancer stem cells, blocking their contributions to hepatocellular carcinoma. *Cancer Res* 2012; **72**: 4276–4285.
- Piccirillo SG, Reynolds BA, Zanetti N, Lamorte G, Binda E, Broggi G *et al*. Bone morphogenetic proteins inhibit the tumorigenic potential of human brain tumour-initiating cells. *Nature* 2006; **444**: 761–765.
- Wang L, Park P, Zhang H, La Marca F, Claesson A, Than K *et al*. BMP-2 inhibits tumor growth of human renal cell carcinoma and induces bone formation. *Int J Cancer* 2012; **131**: 1941–1950.

- 27 Virtanen S, Alarmo EL, Sandstrom S, Ampuja M, Kallioniemi A. Bone morphogenetic protein -4 and -5 in pancreatic cancer—novel bidirectional players. *Exp Cell Res* 2011; **317**: 2136–2146.
- 28 Hahn SA, Seymour AB, Hoque AT, Schutte M, da Costa LT, Redston MS *et al*. Allelotype of pancreatic adenocarcinoma using xenograft enrichment. *Cancer Res* 1995; **55**: 4670–4675.
- 29 Hahn SA, Schutte M, Hoque AT, Moskaluk CA, da Costa LT, Rozenblum E *et al*. DPC4, a candidate tumor suppressor gene at human chromosome 18q21.1. *Science* 1996; **271**: 350–353.
- 30 Thiagalingam S, Lengauer C, Leach FS, Schutte M, Hahn SA, Overhauser J *et al*. Evaluation of candidate tumour suppressor genes on chromosome 18 in colorectal cancers. *Nat Genet* 1996; **13**: 343–346.
- 31 Kang YK, Kim WH, Jang JJ. Expression of G1-S modulators (p53, p16, p27, cyclin D1, Rb) and Smad4/Dpc4 in intrahepatic cholangiocarcinoma. *Hum Pathol* 2002; **33**: 877–883.
- 32 Yao L, Li FJ, Tang ZQ, Gao S, Wu QQ. Smad4 expression in hepatocellular carcinoma differs by hepatitis status. *Asian Pac J Cancer Prev* 2012; **13**: 1297–1303.
- 33 Hiwatashi K, Ueno S, Sakoda M, Kubo F, Tateno T, Kurahara H *et al*. Strong Smad4 expression correlates with poor prognosis after surgery in patients with hepatocellular carcinoma. *Ann Surg Oncol* 2009; **16**: 3176–3182.
- 34 Kodach LL, Bleuming SA, Peppelenbosch MP, Hommes DW, van den Brink GR, Hardwick JC. The effect of statins in colorectal cancer is mediated through the bone morphogenetic protein pathway. *Gastroenterology* 2007; **133**: 1272–1281.
- 35 Kodach LL, Bleuming SA, Musler AR, Peppelenbosch MP, Hommes DW, van den Brink GR *et al*. The bone morphogenetic protein pathway is active in human colon adenomas and inactivated in colorectal cancer. *Cancer* 2008; **112**: 300–306.
- 36 Guo X, Wang XF. Signaling cross-talk between TGF-beta/BMP and other pathways. *Cell Res* 2009; **19**: 71–88.
- 37 Piek E, Roberts AB. Suppressor and oncogenic roles of transforming growth factor-beta and its signaling pathways in tumorigenesis. *Adv Cancer Res* 2001; **83**: 1–54.
- 38 Mullauer L, Grasl-Kraupp B, Bursch W, Schulte-Hermann R. Transforming growth factor beta 1-induced cell death in preneoplastic foci of rat liver and sensitization by the antiestrogen tamoxifen. *Hepatology* 1996; **23**: 840–847.
- 39 Abou-Shady M, Baer HU, Friess H, Berberat P, Zimmermann A, Graber H *et al*. Transforming growth factor betas and their signaling receptors in human hepatocellular carcinoma. *Am J Surg* 1999; **177**: 209–215.
- 40 Matsuzaki K, Kitano C, Murata M, Sekimoto G, Yoshida K, Uemura Y *et al*. Smad2 and Smad3 phosphorylated at both linker and COOH-terminal regions transmit malignant TGF-beta signal in later stages of human colorectal cancer. *Cancer Res* 2009; **69**: 5321–5330.
- 41 Thawani JP, Wang AC, Than KD, Lin CY, La Marca F, Park P. Bone morphogenetic proteins and cancer: review of the literature. *Neurosurgery* 2010; **66**: 233–246 discussion 246.
- 42 Maegdefrau U, Bosserhoff AK. BMP activated Smad signaling strongly promotes migration and invasion of hepatocellular carcinoma cells. *Exp Mol Pathol* 2012; **92**: 74–81.
- 43 Chiu CY, Kuo KK, Kuo TL, Lee KT, Cheng KH. The activation of MEK/ERK signaling pathway by bone morphogenetic protein 4 to increase hepatocellular carcinoma cell proliferation and migration. *Mol Cancer Res* 2012; **10**: 415–427.
- 44 Carreira AC, Lojudice FH, Halcsik E, Navarro RD, Sogayar MC, Granjeiro JM. Bone morphogenetic proteins: facts, challenges, and future perspectives. *J Dent Res* 2014; **93**: 335–345.
- 45 Sakai H, Furihata M, Matsuda C, Takahashi M, Miyazaki H, Konakahara T *et al*. Augmented autocrine bone morphogenetic protein (BMP) 7 signaling increases the metastatic potential of mouse breast cancer cells. *Clin Exp Metastasis* 2012; **29**: 327–338.
- 46 Li Q, Gu X, Weng H, Ghafoory S, Liu Y, Feng T *et al*. Bone morphogenetic protein-9 induces epithelial to mesenchymal transition in hepatocellular carcinoma cells. *Cancer Sci* 2013; **104**: 398–408.
- 47 Pedroza-Gonzalez A, Verhoef C, Ijzermans JN, Peppelenbosch MP, Kwekkeboom J, Verheij J *et al*. Activated tumor-infiltrating CD4+ regulatory T cells restrain anti-tumor immunity in patients with primary or metastatic liver cancer. *Hepatology* 2013; **57**: 183–194.
- 48 Hernanda PY, Pedroza-Gonzalez A, van der Laan LJ, Broker ME, Hoogduijn MJ, Ijzermans JN *et al*. Tumor promotion through the mesenchymal stem cell compartment in human hepatocellular carcinoma. *Carcinogenesis* 2013; **34**: 2330–2340.
- 49 Pan Q, de Ruiter PE, von Eije KJ, Smits R, Kwekkeboom J, Tilanus HW *et al*. Disturbance of the microRNA pathway by commonly used lentiviral shRNA libraries limits the application for screening host factors involved in hepatitis C virus infection. *FEBS Lett* 2011; **585**: 1025–1030.
- 50 van Horssen R, Galjart N, Rens JA, Eggermont AM, ten Hagen TL. Differential effects of matrix and growth factors on endothelial and fibroblast motility: application of a modified cell migration assay. *J Cell Biochem* 2006; **99**: 1536–1552.
- 51 Das AM, Seynhaeve AL, Rens JA, Vermeulen CE, Koning GA, Eggermont AM *et al*. Differential TIMP3 expression affects tumor progression and angiogenesis in melanomas through regulation of directionally persistent endothelial cell migration. *Angiogenesis* 2014; **17**: 163–177.
- 52 Pan Q, Liu B, Liu J, Cai R, Liu X, Qian C. Synergistic antitumor activity of XIAP-shRNA and TRAIL expressed by oncolytic adenoviruses in experimental HCC. *Acta Oncol* 2008; **47**: 135–144.

Supplementary Information accompanies this paper on the Oncogene website (<http://www.nature.com/onc>)

## Supplementary Information

### Supplementary Figure 1

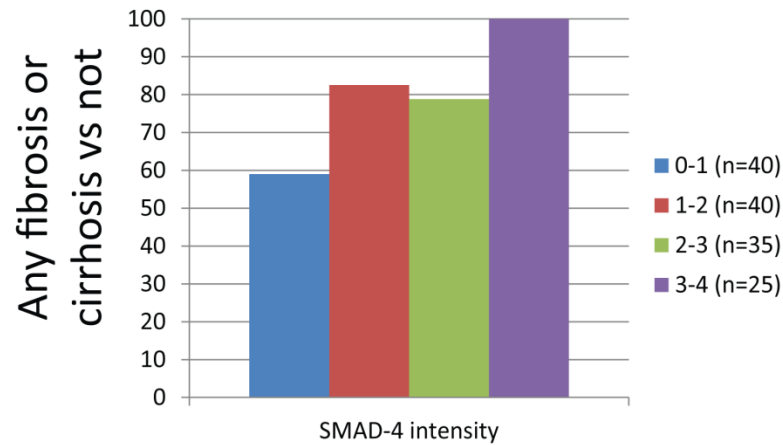


**Figure S1.** SMAD4 is significantly associated with liver fibrosis. Score 0 for 0-10% positive staining, score 1 for 10-30% positive staining, score 2 for 30-70% positive staining, score 3 for >70% positive staining, and score 4 for >70% positive staining. 0-1 represents any score from 0 to (including) 1; 1-2 represents any score higher than 1 and up to 2; 2-3 represents any score higher than 2 and up to 3; 3-4 represents any score higher than 3 and up to 4.  $P < 0.01$ ; Chi-Square test.



## Supplementary Figure 2

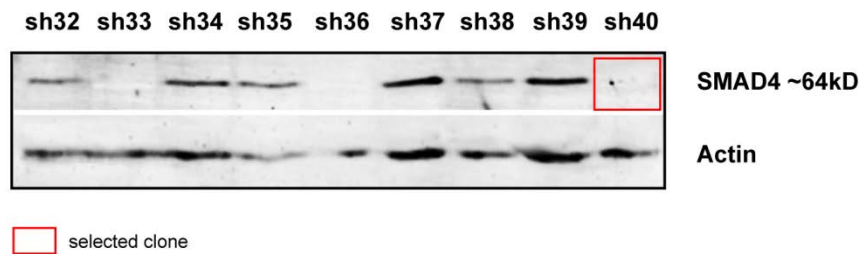
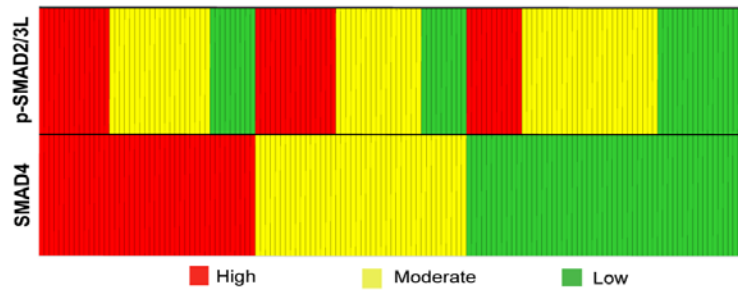


**Figure S2.** Selection of optimal lentiviral shRNA vectors for targeting SMAD4. Western blotting was used to evaluate the efficacy of SMAD4 knockdown in Huh7, Huh6 and PLC cells. Sh40 was selected for follow-up experimentation.

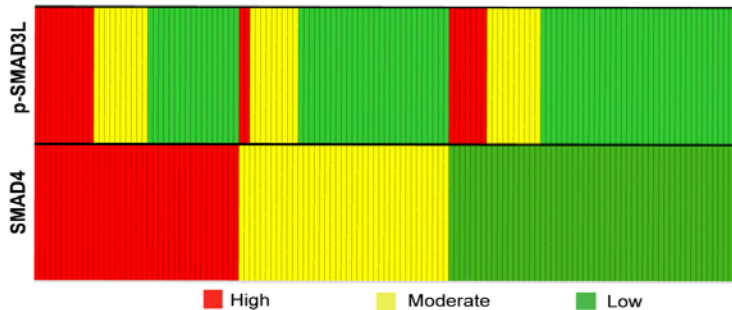
## Supplementary Figure 3

**A**



		P-SMAD2/3L Level			Total
		Low	Moderate	High	
SMAD4 Level	Low	17 48,6%	27 42,2%	11 26,8%	55 39,3%
	Moderate	9 25,7%	17 26,6%	16 39,0%	42 30,0%
	High	9 25,7%	20 31,2%	14 34,1%	43 30,7%
Total		35 100,0%	64 100,0%	41 100,0%	140 100,0%

**B**



		P-SMAD3L Level			Total
		Low	Moderate	High	
SMAD4 Level	Low	37 45,1%	10 34,5%	7 35,0%	54 41,2%
	Moderate	28 34,1%	9 31,0%	2 10,0%	39 29,8%
	High	17 20,7%	10 34,5%	11 55,0%	38 29,0%
Total		82 100,0%	29 100,0%	20 100,0%	131 100,0%

**Figure S3.** The expression level of SMAD4 together with p-SMAD2/3L (A) and p-SMAD3L (B) in our HCC cohort and its cross tabulation.

#### Supplementary Figure 4

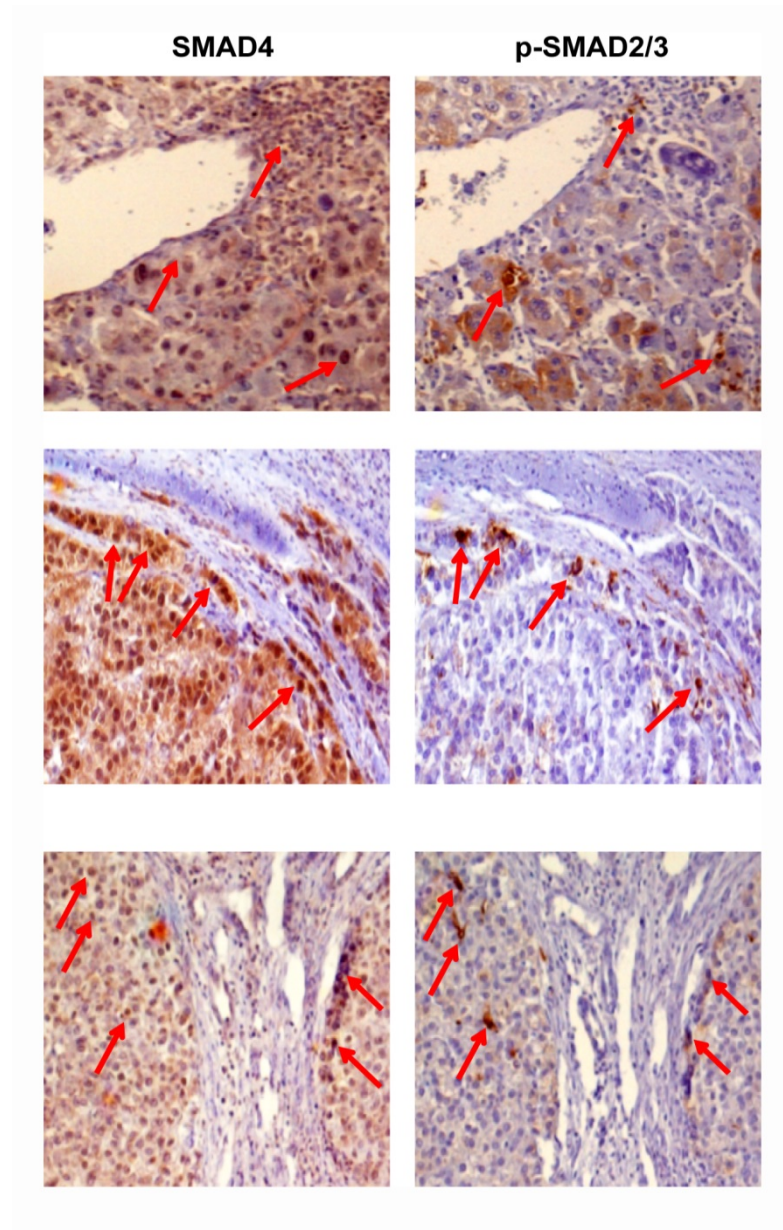


**Figure S4.** Immunohistochemistry staining of SMAD4 and p-SMAD2/3C in consecutive tissue slices of HCC patient





**Supplementary Table S1** Patient characteristics according to SMAD4 expression level.

No	Characteristics	SMAD4 expression		Total patients	P-value <sup>a</sup>
		Low-mod	High		
1	Age	60.70 ± 15.62	59.88 ± 12.61	140/140	0.763
2	Sex (% male)	68/97 (70.1%)	29/43 (67.4%)	97/140	0.753
3	Recurrence	32/97 (33,0%)	15/43 (34.9%)	47/140	0.827
4	Death	30/97 (30,9%)	14/43 (32.6%)	44/140	0.848
5	Size of tumor	6.88 ± 0.63	6.55 ± 0.99	98/140	0.777
6	Number of lesions	1.56 ± 0.11	1.39 ± 0.17	129/140	0.413
7	Vascular invasion	54/85 (63.5%)	24/36 (66.7%)	78/140	0.742
8	AFP before resection**	5.00	16.00	135/140	0.005

\*\*P value < 0.01

<sup>a</sup>Categorized parameters were compared using Pearson's Chi-Square test, mean differences were tested using Student's *t*-test, median differences were tested using Mann-Whitney test

**Supplementary Table S2** Patient characteristics according to p-SMAD2/3C expression level.

No	Characteristics	p-SMAD2/3C expression		Total Patients	P-value <sup>a</sup>
		Low-mod	High		
1	Age	58.71 ± 15.76	63.22 ± 12.56	140/140	0.077
2	Sex (% male)	57/86 (66.3%)	40/54 (74.1%)	97/140	0.330
3	Recurrence*	23/86 (26.7%)	24/54 (44.4%)	47/140	0.031
4	Death*	21/86 (24.4%)	23/54 (42.6%)	44/140	0.024
5	Size of tumor	6.68 ± 5.38	6.97 ± 5.13	98/140	0.796
6	Number of lesions	1.44 ± 1.00	1.6 ± 1.20	129/140	0.376
7	Vascular invasion	51/74 (68.9%)	27/47 (57.4%)	78/140	0.199
8	AFP before resection	10.00	7.00	135/140	0.077

\*P value < 0.05

<sup>a</sup>Categorized parameters were compared using Pearson's Chi-Square test, mean differences were tested using Student's *t*-test, median differences were tested using Mann-Whitney test

**Supplementary Table S3** Patient characteristics according to p-SMAD2/3L expression level.

No	Characteristics	p-SMAD2/3L expression		Total Patients	P-value <sup>a</sup>
		Low-mod	High		
1	Age	61.42 ± 13.12	58.10 ± 17.98	140/140	0.225
2	Sex (% male)	72/99 (72.7%)	25/41 (61.0%)	97/140	0.170
3	Recurrence	34/99 (34.3%)	13/41 (31.7%)	47/140	0.764
4	Death	30/99 (30.3%)	14/41 (34.1%)	44/140	0.656
5	Size of tumor	6.74 ± 4.89	6.90 ± 6.14	98/140	0.893
6	Number of lesions	1.54 ± 1.09	1.41 ± 1.07	129/140	0.520
7	Vascular invasion	56/84 (66.7%)	22/37 (59.5%)	78/140	0.445
8	AFP before resection	11.00	7.00	135/140	0.343

<sup>a</sup>Categorized parameters were compared using Pearson's Chi-Square test, mean differences were tested using Student's *t*-test, median differences were tested using Mann-Whitney test

**Supplementary Table S4** Patient characteristics according to p-SMAD3L expression level.

No	Characteristics	p-SMAD3L level		Total Patients	P-value <sup>a</sup>
		No	Yes		
1	Age	60.77 ± 15.00	60.25 ± 14.46	140/140	0.885
2	Sex (% male)	80/111 (72.1%)	11/20 (55.0%)	97/140	0.127
3	Recurrence	37/111 (33.3%)	8/20 (40.0%)	47/140	0.563
4	Death	32/111 (28.8%)	9/20 (45%)	44/140	0.151
5	Size of tumor	6.92 ± 5.34	6.83 ± 5.27	98/140	0.957
6	Number of lesions	1.55 ± 1.15	1.24 ± 0.56	129/140	0.080
7	Vascular invasion	62/95 (65.3%)	10/17 (58.8%)	78/140	0.610
8	AFP before resection	7.00	16.00	135/140	0.658

<sup>a</sup>Categorized parameters were compared using Pearson's Chi-Square test, mean differences were tested using Student's *t*-test, median differences were tested using Mann-Whitney test

**Supplementary Table S5** Patient characteristics according to high SMAD4 expression and moderate-high p-SMAD2/3C expression level.

No	Characteristics	High SMAD4 + HighMod p-SMAD2/3C level		Total Patients	P-value <sup>a</sup>
		No	Yes		
1	Age	61.04 ± 15.45	57.85 ± 10.82	140/140	0.319
2	Sex (% male)	80/114 (70.2%)	17/26 (65.4%)	97/140	0.633
3	Recurrence	35/114 (30.7%)	12/26 (46.2%)	47/140	0.132
4	Death	34/114 (29.8%)	10/26 (38.5%)	44/140	0.392
5	Size of tumor	6.85 ± 5.23	6.50 ± 5.53	98/140	0.800
6	Number of lesions	1.52 ± 1.08	1.44 ± 1.12	129/140	0.744
7	Vascular invasion	67/100 (67%)	11/21 (52.4%)	78/140	0.203
8	AFP before resection	6.50	14.00	135/140	0.136

<sup>a</sup>Categorized parameters were compared using Pearson's Chi-Square test, mean differences were tested using Student's *t*-test, median differences were tested using Mann-Whitney test



**Supplementary Table S6** Patient characteristics according to high SMAD4 expression and moderate-high p-SMAD2/3L expression level.

No	Characteristics	High SMAD4 + ModHigh p-SMAD2/3L level		Total Patients	P-value <sup>a</sup>
		No	Yes		
1	Age	60.92 ± 15.23	58.96 ± 13.18	140/140	0.503
2	Sex (% male)	76/106 (71.7%)	21/34 (61.8%)	97/140	0.275
3	Recurrence	36/106 (34.0%)	11/34 (32.4%)	47/140	0.863
4	Death	31/106 (29.2%)	13/34 (38.2%)	44/140	0.392
5	Size of tumor	6.89 ± 5.32	6.48 ± 5.12	98/140	0.738
6	Number of lesions	1.52 ± 1.04	1.47 ± 1.22	129/140	0.831
7	Vascular invasion	58/91 (63.7%)	20/30 (66.7%)	78/140	0.771
8	AFP before resection**	5.50	27.00	135/140	0.004

\*\*P value < 0.01

<sup>a</sup>Categorized parameters were compared using Pearson's Chi-Square test, mean differences were tested using Student's *t*-test, median differences were tested using Mann-Whitney test

**Supplementary Table S7** Patient characteristics according to high SMAD4 expression and moderate-high p-SMAD3C expression level.

No	Characteristics	High SMAD4 + ModHigh p-SMAD3C level		Total Patients	P-value <sup>a</sup>
		No	Yes		
1	Age	60.54 ± 15.00	59.67 ± 14.06	140/140	0.804
2	Sex (% male)	81/114 (71.1%)	12/21 (57.1%)	97/140	0.206
3	Recurrence	38/114 (33.3%)	7/21 (33.3%)	47/140	1.000
4	Death	35/114 (30.7%)	8/21 (38.1%)	44/140	0.504
5	Size of tumor	6.58 ± 5.12	8.14 ± 6.26	98/140	0.313
6	Number of lesions	1.59 ± 1.16	1.06 ± 0.23	129/140	0.054
7	Vascular invasion	63/98 (64.3%)	12/18 (66.7%)	78/140	0.846
8	AFP before resection	6.50	13.50	135/140	0.154

<sup>a</sup>Categorized parameters were compared using Pearson's Chi-Square test, mean differences were tested using Student's *t*-test, median differences were tested using Mann-Whitney test

**Supplementary Table S8** Patient characteristics according to p-SMAD1/5/8 expression level.

No	Characteristics	p-SMAD1/5/8 expression		Total Patients	P-value <sup>a</sup>
		Low-mod	High		
1	Age***	62.24 ± 11.96	47.53 ± 24.29	140/140	0.000
2	Sex (% male)	88/123 (71.5%)	9/17 (52.9%)	97/140	0.119
3	Recurrence	43/123 (35,0%)	4/17 (23.5%)	47/140	0.350
4	Death	40/123 (32.5%)	4/17 (23.5%)	44/140	0.454
5	Size of tumor	6.70 ± 5.14	7.45 ± 6.38	98/140	0.657
6	Number of lesions	1.50 ± 1.07	1.41 ± 1.23	129/140	0.708
7	Vascular invasion	70/105 (66.7%)	78/121 (64.5%)	78/140	0.194
8	AFP before resection	8.00	7.50	135/140	0.664

\*\*\*P value < 0.001

<sup>a</sup>Categorized parameters were compared using Pearson's Chi-Square test, mean differences were tested using Student's *t*-test, median differences were tested using Mann-Whitney test